Computational and Theoretical Chemistry 1203 (2021) 113330

Contents lists available at ScienceDirect

Computational and Theoretical Chemistry

journal homepage: www.elsevier.com/locate/comptc

Non-uniform heat source/sink applications for the radiative flow of Brinkman micropolar nanofluid with microorganisms

Kamel Al-Khaled [a], M. Ijaz Khan [b,c,*], Sami Ullah Khan [d], M.Y. Malik [e], Sumaira Qayyum [f]

[a] Department of Mathematics & Statistics, Jordan University of Science and Technology, P.O. Box 3030, Irbid 22110, Jordan
[b] Department of Mathematics and Statistics, Riphah International University I-14, Islamabad, Pakistan
[c] Nonlinear Analysis and Applied Mathematics (NAAM)-Research Group, Department of Mathematics, Faculty of Sciences, King Abdulaziz University, P.O. Box 80203, Jeddah 21589, Saudi Arabia
[d] Department of Mathematics, COMSATS University Islamabad, Sahiwal 57000, Pakistan
[e] Department of Mathematics, College of Sciences, King Khalid University, Abha 61413, Saudi Arabia
[f] Department of Mathematics, Quaid-I-Azam University, 45320, Islamabad 44000, Pakistan

ARTICLE INFO

Keywords:
Bioconvection flow
Heat and mass transfer
Brinkman micropolar nanofluid
Numerical scheme

ABSTRACT

The thermal consequences of the Brinkman type micropolar nanoparticles are inspected theoretically in presence of microorganisms. The impact of non-uniform heat source and sink is also observed. The thermo-diffusion aspects of nano-materials are visualized for heat and mass transfer phenomenon. The appropriate transformations successfully convert the flow problem into dimensionless form. The shooting numerical computations are performed to access the solution. The accuracy of numerical data is predicted via making comparison with already performed continuations. The graphical significances for the desired parameters is addressed with aims for graphs and tables. The findings are summarized with practical applications. The novel outcomes show that velocity of fluid reduces with inclination factor and Brinkman parameter. The nanofluid temperature is enhanced with non-uniform heat source sink parameters and Brinkman parameter. The nanofluid concentration reduces with viscosity constraint. The obtained results presents applications in the era of thermal engineering, energy production, cooling and heat systems, enzymes etc.

1. Introduction

Owing to the dynamic evolution in the thermal sciences and modern nanotechnology, the scientists has presented the idea of nanofluids with ultra-high thermal properties. With multidisciplinary applications, the researchers have presented many valuable contributions on the flow of nanofluids with extra ordinary thermal activities. The nanofluids are assumed to be a uniform immersion of nanoparticles in the base liquids which discover a fundamental improvement in the heat fluctuation phenomenon. With high dynamic thermal activities, the interaction of nanoparticles helps to fulfill the requirement of energy in various engineering and industrial processes. The applications which reflected from the nanofluids include in many era of sciences, medical engineering, industries, biomedicine, technologies and thermal engineering. The base liquids which use as a source of energy in much industrial mechanism are improved with interaction of nanoparticles. With nano-size diameter (1–100 nm), the nanoparticles attributed major importance in energy production, nano-materials, metallurgical phenomenon, cooling of devices electronics, controlled drug delivery, chemical processes etc. Choi [1] discussed the basic work on nanofluids by reporting the experimental explanations. The thermophoresis and Brownian approach for the nanofluids flow was pointed out by Buongiorno [2]. Ibrahim et al. [3] determined the thermal mechanism of Williamson nanofluid when the melting phenomenon and dissipation features were more progressive. Acharya et al. [4] addressed the magnetic force impact on the thermal properties of nanofluid assumed in directional moving surface. Acharya [5] performed the computational analysis for the nanoparticles flow with multiple convective constraints and radiation influence. Wasqas et al. [6] explored the thermal prospective of Maxwell and micropolar nanoparticles in a porous space. Acharya and Mabood [7] pointed out the distinct thermal applications of Fe_3O_4 hybrid nanoparticles due to heat generation features over slippery surface. Acharya et al. [8] discussed the improvement in heat transfer by using the nanofluids and radiation phenomenon. Hashmi et al. [9]

* Corresponding author at: Department of Mathematics and Statistics, Riphah International University I-14, Islamabad, Pakistan.
E-mail address: mikhan@math.qau.edu.pk (M.I. Khan).

https://doi.org/10.1016/j.comptc.2021.113330
Received 11 March 2021; Received in revised form 1 June 2021; Accepted 7 June 2021
Available online 10 June 2021

Table 1

Comparison table for $\left(1+\frac{K}{2}\right)f''(0)$ when $\lambda = \beta_m = Nr = Rb = 0$.

K	Turkyilmazoglu [22]	Present results
0.0	−1.00000000	−1.00000000
1.0	−1.22474487	−1.22474485
2.0	−1.41421356	−1.41421352

studied the thermophoretic decomposition of Maxwell nanofluid confined by moving disks. Acharya et al. [10] examined the effects of slip and convective conditions impact for the nanofluid flow by performing the statistical analysis. The investigation addressed by Khan [11] conveys the hybrid nanofluid properties assumed due to rotating disk flow. Ramesh et al. [12] presented the convective thermal mode of Al_2O_3-Ag nanoparticles numerically via shooting approach. Rafique [13] performed the thermal simulations for the Brinkman micropolar nanofluid with thermophoresis applications. Khan and Alzahrani determined the convective transport of silicon dioxide and molybdenum disulfide nanoparticles with entropy generation pattern for the Sisko liquid. The bioconvection phenomenon is the most valuable the impressive research area in the bio-engineering and bio-technology. The bioconvection phenomenon is usually assumed as a sub branch of thermofluid which reflects the applications of convective transport of nano-materials in presence of microorganisms. The bio-convective transport pattern is associated with the hydrodynamic instability for the upward flow of microorganisms which float in the upper zone of the surface. The microorganisms have properties to throw out in distinct surrounding consequences like gravitational force, chemical reaction, electric and magnetic force. The nanoparticles flow the Brownian and thermophoretic mechanism as compared to the microorganism which are self oriented. The bioconvection phenomenon presents the distinct applications in bio-fuels, bacteria, fertilizers etc. Kuznetsov [15] worked out the mathematical modeling of bioconvection problem and discussed the oxytactic microorganisms phenomenon. Makinde and Animasaun [16] addressed the bioconvection pattern with quartic autocatalysis and fundamental features of thermal radiation and chemical reaction. Acharya et al. [17] claimed the applications of solar radiation for bioconvection magnetized flow of nanofluid. The work performed by Acharya et al. [18] evaluated the role of slip factor for nanofluid flow with microorganisms. Usman et al. [19] addressed the Eyring Powell bioconvection flow proflem due to Riga transport by exploring the nonlinear thermal radiation phenomenon. Nadeem et al. [20] discussed a computational problem for the ferrofluid flow with microorganisms numerically. The finite element numerical approach for micropolar nanofluid fluid was followed by Ali et al. [21].

The bioconvection applications in chemical reactive flow of Brinkman micropolar nanofluid over inclined surface is examined numerically in this contribution. The magnetic force, activation energy and thermal radiation phenomenon is also encountered. Moreover, the non-uniform heat absorption and generation consequences are entertained to improve the progressive heat transportation prospective. The convective Nield conditions for the formulated problem are convinced to perform the analysis. The numerical shooting technique is imposed to address the solution procedure.

2. Flow analysis

The convective transport of Brinkman micropolar is visualized in presence of microorganism. The inclined surface induced the flow with uniform velocity. The associated thermal relations for the non-uniform heat source/sink, thermal radiation and activation energy are intro-

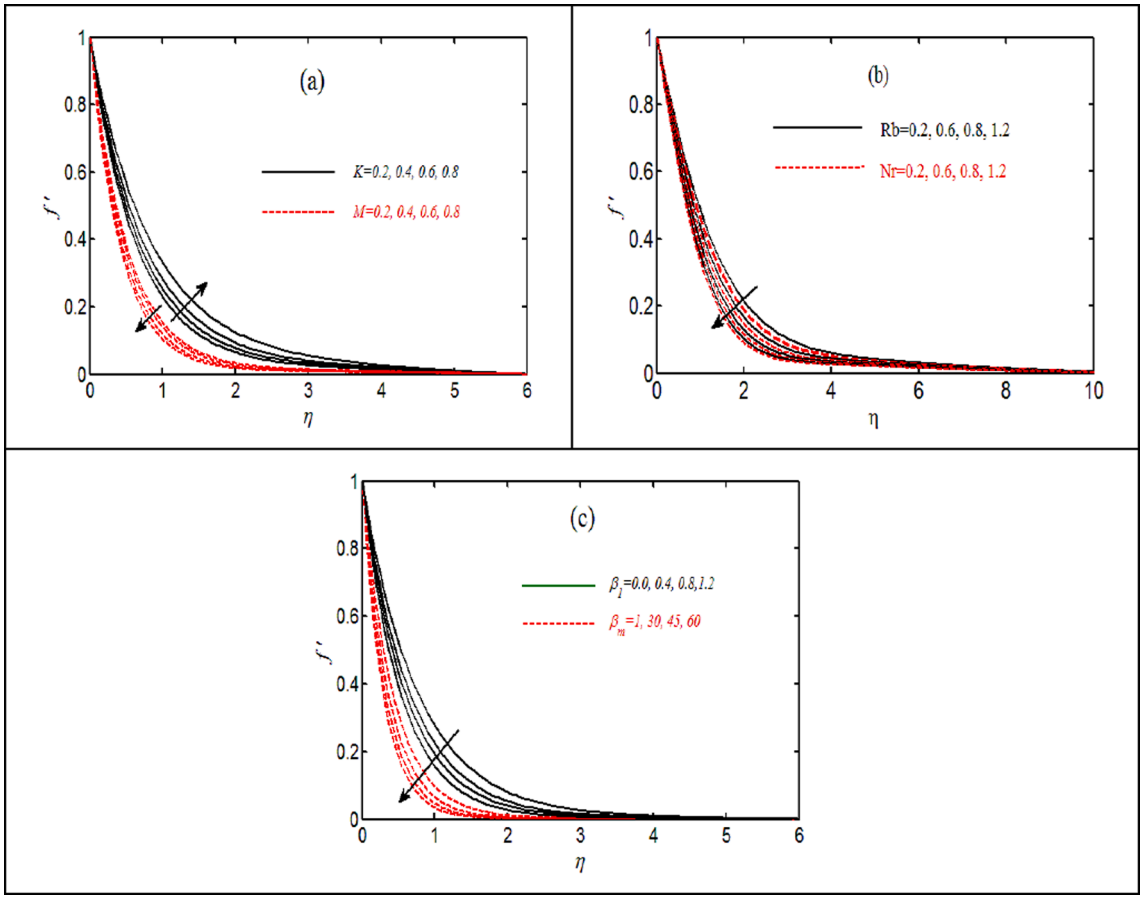

Fig. 1. (a-c): Velocity profile for (a) parameter M and K (b) Rb and Nr. (c) β_m and factor β_1

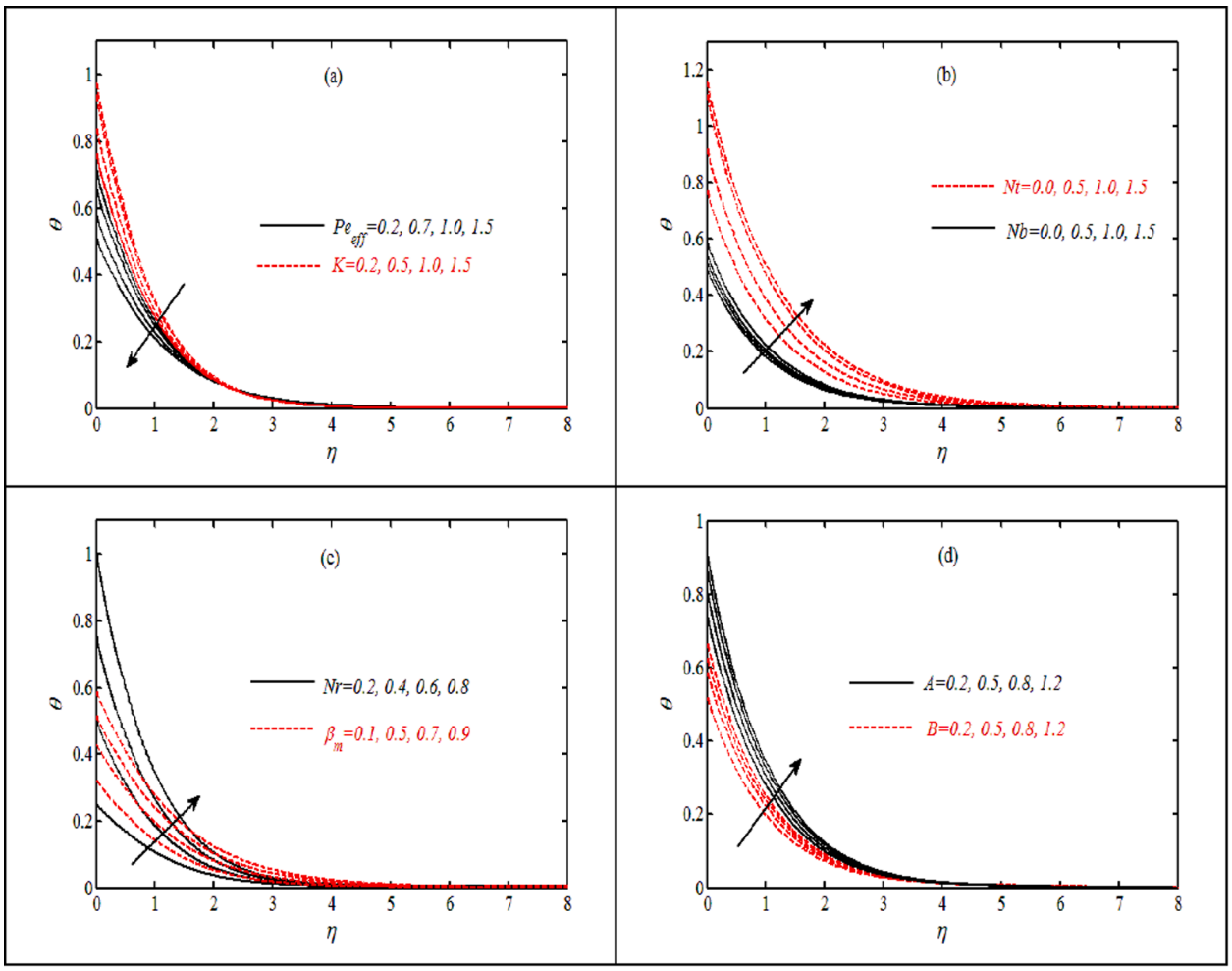

Fig. 2. (a-d): Temperature profile for (a) Pr_{eff} and K, (b) Nt and Nb, (c) Nr and β_m (d) A and B.

duced to modify the heat and concentration equations. The magnetic force implementation is followed for electrically conducting micropolar nanofluid. The cartesian system is allowed to access the flow modeling. The uniform velocity of the considered inclined surface is expressed with $u_w(x) = ax$. The velocity components normal to flow and along the flow are symbolized with u and v, respectively. The governing equations representing the Brinkman type micropolar nanofluid with described flow features are represented in the following form [13,21]:

$$\frac{\partial u}{\partial x}+\frac{\partial v}{\partial y}=0, \tag{1}$$

$$u\frac{\partial u}{\partial x}+v\frac{\partial u}{\partial y}=\left(\frac{\mu+k_1}{\rho_f}\right)\frac{\partial^2 u}{\partial y^2}+\frac{k_1}{\rho_f}\frac{\partial N^*}{\partial y}-\left(\frac{\sigma^* B_0^2}{\rho_f}-\beta^*\right)u+\frac{1}{\rho_f}\left[\begin{array}{c}(1-c_\infty)\rho_f\Omega^* g_1(T-T_\infty)-(\rho_p-\rho_f)g_1(c-c_\infty)\\ -(n-n_\infty)g_1\gamma^*(\rho_m-\rho_f)\end{array}\right]cos\beta_1, \tag{2}$$

$$\left(u\frac{\partial N^*}{\partial x}+v\frac{\partial N^*}{\partial y}\right)=\frac{\gamma^*}{\rho_f j^*}\left(\frac{\partial^2 N^*}{\partial y^2}\right)-\frac{k_1}{\rho_f j^*}\left(2N^*+\frac{\partial u}{\partial y}\right), \tag{3}$$

$$u\frac{\partial T}{\partial x}+v\frac{\partial T}{\partial y}=\left(\alpha_c+\frac{16\sigma_r T_\infty^3}{3(\rho c)_f k^*}\right)\frac{\partial^2 T}{\partial y^2}+\Lambda_w\left(\frac{D_T}{T_\infty}\left(\frac{\partial T}{\partial y}\right)^2+D_B\left(\frac{\partial C}{\partial y}\frac{\partial T}{\partial y}\right)\right)+\frac{Q_c}{(\rho c)_f}, \tag{4}$$

$$u\frac{\partial c}{\partial x}+v\frac{\partial c}{\partial y}=D_B\frac{\partial^2 c}{\partial y^2}-kr^2(c-c_\infty)\left(\frac{T}{T_\infty}\right)^m exp\left(\frac{-E_a}{kT}\right)+\frac{D_T}{T_\infty}\frac{\partial^2 T}{\partial y^2}, \tag{5}$$

$$u\frac{\partial n}{\partial x}+v\frac{\partial n}{\partial y}+\frac{b_m w_m}{(c_w-c_\infty)}\frac{\partial}{\partial y}\left(n\frac{\partial c}{\partial y}\right)=D_m\frac{\partial^2 n}{\partial y^2}, \tag{6}$$

The expressions for the non-uniform heat source and sink Q_c are presented as:

$$Q_c=\frac{KU_w}{x\nu}\left(A_1(T_f-T_\infty)f'+B_1(T-T_\infty)\right), \tag{7}$$

The boundary conditions are [13,21]:

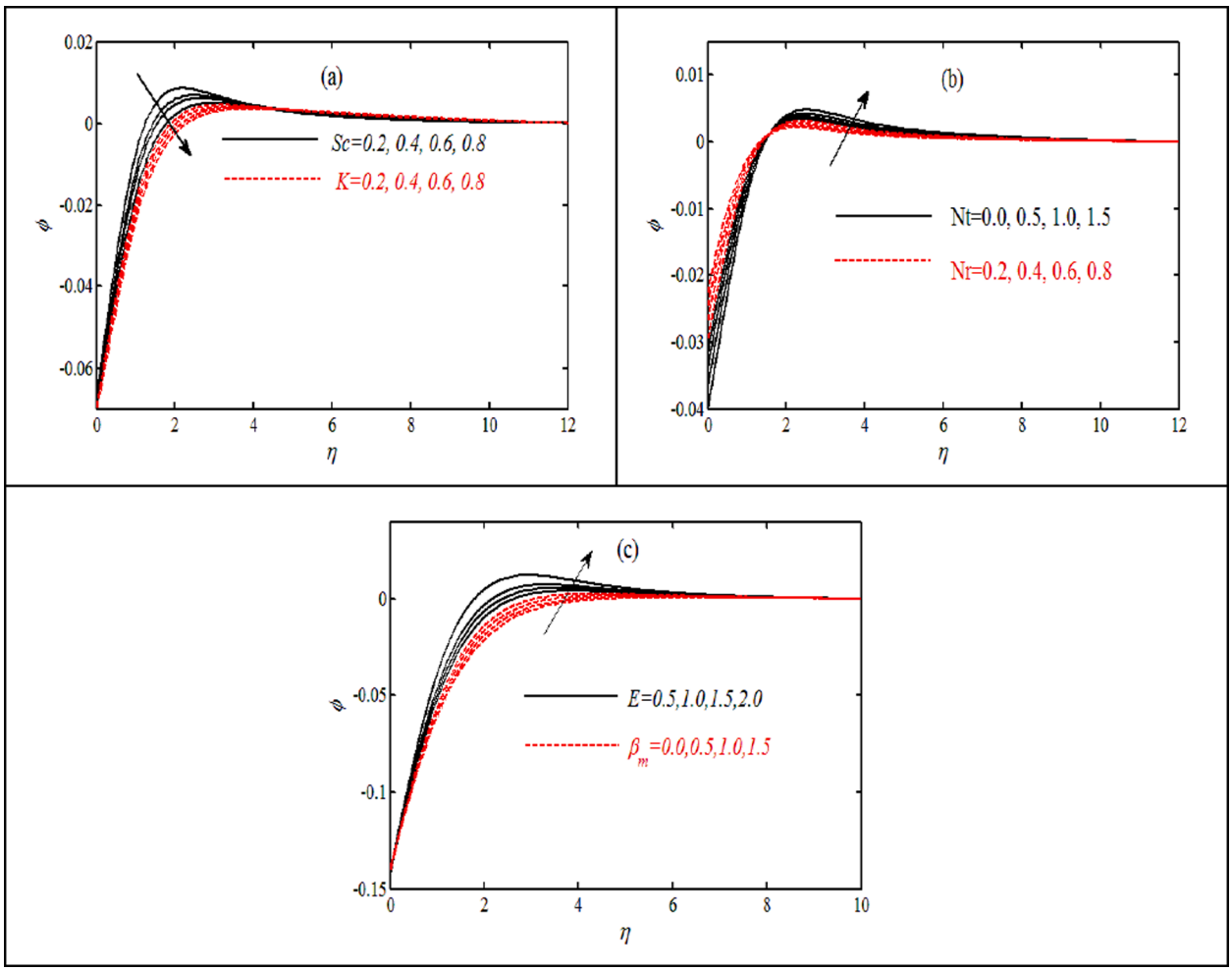

Fig. 3. (a-c): Concentration profile for (a) *Sc* and *K*, (b) *Nt* and *Nr*, (c) *E* and β_m.

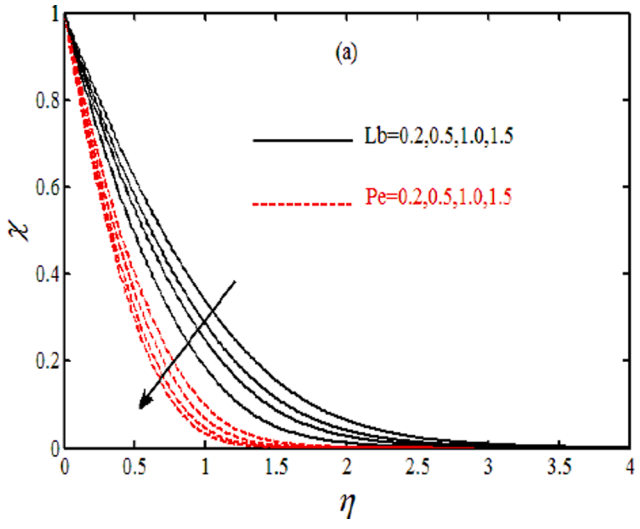

Fig. 4. Microorganism profile for *Lb* and *Pe*..

$$u = u_w,\ v = 0,\ N^* = -m_0^* \frac{\partial u}{\partial y},\ -k\frac{\partial T}{\partial y} = h_f(T_w - T),\ D_B\frac{\partial c}{\partial y} + \frac{D_T}{T_\infty}\frac{\partial T}{\partial y} = 0,\ n = n_w, \tag{8}$$

$$u \to u_\infty(x) = 0,\quad N^* \to 0, T \to T_\infty, c \to c_\infty, n \to n_\infty \ as\ y \to \infty. \tag{9}$$

Table 2
Numerical values of $-\theta'(0)$, $-\phi'(0)$, $-\chi'(0)$.

K	*Nt*	*Nb*	β_1	$-\theta'(0)$	$-\phi'(0)$	$-\chi'(0)$
0.1	0.2	0.2	30	0.35	0.48	0.55
0.5				0.37	0.50	0.59
0.7				0.41	0.52	0.60
0.3	0.1			0.33	0.45	0.57
	0.3			0.32	0.41	0.53
	0.5			0.30	0.38	0.51
		0.1		0.37	0.42	0.50
		0.5		0.35	0.45	0.47
		0.7		0.31	0.48	0.42
			45	0.40	0.45	0.51
			60	0.38	0.42	0.49

The physical quantities are ρ_f (fluid density), σ^* (electric conductivity), μ (viscosity), B_0 (magnetic field strength), N^* (micro-rotation), j^* (micro-inertia), β^* (Brinkman coefficient), ρ_p (nanoparticles density), D_B (Brownian motion coefficient), g_1 (gravity), k_1 (material constant), σ_r (Stefan-Boltzmann coefficient), k^* (mean absorption coefficient), D_T (thermophoresis dispersion), Ω^* (volume suspension coefficient), T (temperature), C (concentration), ρ_m (microorganisms density), n (microorganisms), E_a (energy coefficient), D_m (coefficient of microorganisms), Kr^2 (chemical reaction constant), m (fitted rate constant), m (fitted rate constant), b_m (chemotaxis constant) E_a (activation energy coefficient) and w_m (cell swimming speed)

The developed similarity variables are:

$$\left.\begin{aligned} N^* &= \sqrt{\frac{a}{\nu}}axg(\eta), v = -\sqrt{a\nu}f(\eta), u = axf'(\eta),\ \eta = \sqrt{\frac{a}{\nu}}y,\\ \theta(\eta) &= \frac{T-T_\infty}{T_w-T_\infty},\quad \phi(\eta) = \frac{c-c_\infty}{c_\infty},\quad \chi(\eta) = \frac{n-n_\infty}{n_w-n_\infty}. \end{aligned}\right\} \tag{10}$$

The dimensionless flow problem in view of equations (10) is formulated as:

$$(1+K)f''' + ff'' + Kg' - (f')^2 - (M-\beta_m)f' + \lambda(\theta - Nr\phi - Rb\chi)cos\beta_1 = 0, \tag{11}$$

$$\left(1+\frac{K}{2}\right)g'' - K(2g+f'') - f'g + g'f = 0, \tag{12}$$

$$\left(\frac{1+Rd}{Pr}\right)\theta'' + Pr\left[Nb\theta'\phi' + f\theta' + Nt(\theta')^2\right] + A_1f' + B_1\theta = 0, \tag{13}$$

$$\phi'' - Sc\sigma_c(1+\omega\theta)^m exp\left(-\frac{E}{1+\omega\theta}\right)\phi + \left(\frac{Nt}{Nb}\right)\theta'' + Scf\phi' = 0, \tag{14}$$

$$\chi'' + Lbf\chi' - Pe(\phi''(\chi+\sigma_m) + \chi'\phi') = 0. \tag{15}$$

Eq. (13) is further modified in terms of effective Prandtl number

$$\theta'' + Pr_{eff}\left[Nb\theta'\phi' + f\theta' + Nt(\theta')^2\right] + Pr_{eff}(A_1f' + B_1\theta) = 0, \tag{16}$$

with $Pr_{eff} = (1+Rd)/Pr$

with boundary conditions

$$\left.\begin{aligned} f(0) = 0, f'(0) = 1, g(0) = 0, \theta'(0) = -Bi[1-\theta(0)],\\ Nt\phi'(0) + Nb\theta'(0) = 0, \chi(0) = 1, \end{aligned}\right\} \tag{17}$$

$$f'(\infty)\to 0, g(\infty)\to 0, \theta(\infty)\to 0, \phi(\infty)\to 0, \chi(\infty)\to 0. \tag{18}$$

With flow parameters like vortex viscosity constraint $K = k_1/\rho_f\nu$, magnetic parameter $M = \frac{\sigma^* B_0^2}{a\rho_f}$, Brinkman parameter $\beta_m = \frac{\beta^*}{a}$, bio-convection Rayleigh constant $Rb\left(=\gamma^*(n_w-n_\infty)(\rho_m-\rho_f)/\Omega^*\rho_f(1-C_\infty)(T_w-T_\infty)\right)$, buoyancy ratio constant $Nr\left(=(\rho_p-\rho_f)(C_w-C_\infty)/\Omega^*\rho_f(1-C_\infty)T_\infty\right)$, angular micropolar parameter $\Omega = \frac{K_1^*}{\mu}$, mixed convection parameter $\lambda\left(=\Omega^* g(1-C_\infty)(T_w-T_\infty)/b^2x\right)$, Prandtl number $Pr = \frac{\nu}{\alpha_c}$, Brownian constant $Nb = \frac{\Lambda_w D_B(c_w-c_\infty)}{\alpha_c}$, activation energy $E = E_a/k_aT_\infty$, and radiation parameter $Rd = 4\sigma^* {T_\infty}^3/3kk^*$, thermophoresis constant $Nt = \frac{\Lambda_w D_T(T_w-T_\infty)}{T_\infty\alpha_m}$, Lewis number $Le = \frac{\alpha_m}{D_B}$, bio-convective Lewis number $Lb = \frac{\alpha_c}{D_m}$, activation energy $E\left(=\frac{E^*}{kT_\infty}\right)$, Peclet number $Pe = \frac{b_m w_m}{D_m}$ and motile difference constant $\sigma_m = \frac{n_\infty}{(n_w-n_\infty)}$.

The local Nusselt number, local Sherwood number and motile density number are expressed as:

$$\left.\begin{aligned} \frac{Nu}{\sqrt{Re_x}} &= -\left(1+\frac{4}{3}Rd\right)\theta'(0),\\ \frac{Sh}{\sqrt{Re_x}} &= -\phi'(0),\\ \frac{Nn}{\sqrt{Re_x}} &= -\chi'(0). \end{aligned}\right\} \tag{19}$$

3. Numerical method

The numerical scheme namely shooting technique is employed in this section to discuss the obtained solution. The shooting method is the most effective numerical scheme due to higher accuracy. This method is based on the conversion of boundary value scheme into set of initial value system. This scheme is based on following steps:

$$\left.\begin{aligned} f = s_1, f' = s_2, f'' = s_3, f''' = s_3',\\ g = s_4, g' = s_5, g'' = s_5', \theta = s_6,\\ \theta' = s_7, \theta'' = s_7', \phi = s_8, \phi' = s_9,\\ \phi'' = s_9', \chi = s_{10}, \chi' = s_{11}, \chi'' = s_{11}'. \end{aligned}\right\} \tag{20}$$

$$s_3' = \frac{-(s_1-s_3) + (s_2)^2 + (M-\beta_m)s_2 - \lambda(s_6 - Nrs_8 - Rbs_{10})cos\beta_1}{(1+K)}, \tag{21}$$

$$q_5' = \frac{-q_1q_5 + q_2q_4 + K(2q_4+q_3)}{\left(1+\frac{K}{2}\right)}, \tag{22}$$

$$s_7' = -Pr_{eff}\left[Nbs_7s_9 + s_1s_7 + Nt(s_7)^2\right] - Pr_{eff}(A_1s_2 + B_1s_6), \tag{23}$$

$$s_{11}' = -Scs_1s_{11} - \frac{Nt}{Nb}q_8' + Sc\sigma^{**}(1+\delta s_7)^n q_{11} exp\left(\frac{-E}{1+\delta s_{11}}\right), \tag{24}$$

$$s_{11}' = -Lbs_1s_{11} + Pe(s'_9(\chi+\omega) + s_{11}s_9) \tag{25}$$

with

$$\left.\begin{aligned} s_1(0) = S, s_2(0) = 1, s_4(0) = 0, s_7(0) = -Bi[1-s_6(0)],\\ Nts_9 + Nbs_7 = 0, s_{10} = 1, \end{aligned}\right\} \tag{26}$$

$$s_2(\infty)\to 0,\ s_4(\infty)\to 0,\ s_6(\infty)\to 0,\quad s_8(\infty)\to 0,\ s_{10}(\infty)\to 0. \tag{27}$$

4. Validation of solution

Table 1 presents the solution verification by comparing the obtained numerical data with work of Turkyilmazoglu [22]. A good agreement is noted between both studies.

5. Discussion

The illustration of velocity f' against change magnetic parameter M and viscosity constraint K is inspected by preparing Fig. 1(a). The reduced velocity profile with higher M is noticed. Physically, the increase in magnetic parameter causes a resistive force which is known as Lorentz force. This Lorentz force has tendency to control the increasing change in velocity. The increment in velocity is observed for increasing viscosity constraint K. Physical aspects of such increasing behavior of f' is due to presence of viscous forces. The graphical results reported in Fig. 1(b) visualized the nature of f' for bioconvection Rayleigh constant Rb and buoyancy ratio constant Nr. A reduction in fluid particles velocity for both flow parameters is examined. Physical explanation for such trend is due to presence of buoyancy forces. Fig. 1(c) highlight the influence of Brinkman parameter β_m and inclination factor β_1 on f'. Both parameters effectively presents the resistance in the velocity.

The inspection in temperature θ for increasing variation of Prandtl effective Pr_{eff} and viscosity constraint K has been visualized in Fig. 2(a). With distinct numerical values of Pr_{eff} and K, the temperature profile get decline. The Prandtl effective explored the joint consequences of Prandtl number and radiation constant. The higher change in Prandtl constant depresses the thermal diffusivity due to relation relations between both quantities. The impact of thermophoresis constant Nt and Brownian constant Nb on θ has been presented in Fig. 2(b). Both Brownian motion and thermophoresis constant are the most important parameters of Buongiorno nanofluid model. A boost up nanofluid temperature is raised with both parameters. Physically, the thermophoretic phenomenon presents the motion of heated nanoparticles which moves from heated surface to cooler zone due to temperature gradient. This fluctuation in temperature results improvement in θ. The increasing change in temperature due to Nb is associated to the random movement of fluid particles. Fig. 2(c) explored influence of Nr and β_m on θ. An increasing variation in θ is observed due to Nr and β_m. The results conveyed in Fig. 2 (d) show that nanofluid temperature enhanced with non-uniform heat

source/sink parameters A and B. It is concluded form this results that presence of non-uniform heat source/sink is more effective to improve the nanofluid temperature.

Fig. 3(a) presented the change in concentration ϕ for Schmidt number Sc and viscosity constraint K. The reduction in the profile of ϕ is noticed with Sc. The physical explanation for decrease in ϕ due to Sc is due to the fact that Schmidt number presents the inverse relations with mass diffusivity. The lower mass diffusivity is observed for higher Schmidt number. The impact of K on ϕ also reports decreasing trend. Fig. 3(2) shows that concentration profile arises with thermophoresis constant Nt and buoyancy constant Nr. The graphical results for activation energy E and Brinkman parameter β_m is observed in Fig. 3(c). the presence of both parameters enhanced the concentration. Fig. 4 reposts the influence of bio-convective Lewis number Lb and Peclet number Pe on microorganism profile χ. When Lb and Pe get increasing numerical values, a lower profile of χ is observed. Physically, Peclet number is inversely related to the motile density due to which χ decline.

The numerical values are obtained in table 2 for flow parameters by using the relation of $-\theta'(0), -\phi'(0), -\chi'(0)$. The results predicted from this table show that all physical quantities increases with K while lower numerical values are noticed for β_1 and Nt.

6. Conclusions

The bio-convective significances of Brinkman micropolar nanofluid is addressed in presence of non-uniform heat source/sink and thermal radiation. The shooting technique is used for the solution procedure. The main outcomes observed from current analysis are:

The fluid velocity reduces for the Brinkman parameter and inclination factor.

The nanofluid temperature get enhanced with Brinkman parameter, thermophoresis constant while the results for temperature field are opposite by increasing viscosity constraint.

The presence of non-uniform heat source/sink parameters is more effective to improve the nanofluid temperature.

A lower concentration of nanofluid is inspected with viscosity constraint and Schmidt number.

A boost up concentration profile is predicted with Brinkman parameter.

Declaration of Competing Interest

The authors declare that they have no known competing financial interests or personal relationships that could have appeared to influence the work reported in this paper.

Acknowledgement

The authors extend their appreciation to the Deanship of Scientific Research at King Khalid University, Abha 61413, Saudi Arabia for funding this work through research groups program under grant number R.G.P-1/234/42.

References

[1] S.U.S. Choi, Enhancing thermal conductivity of fluids with nanoparticles, Proc ASME Int, Mech. Eng. Congr. Exposition 66 (1995) 99–105.

[2] J. Buongiorno, Convective transport in nanofluids, J. Heat Transfer 128 (2006) 240–250.

[3] W. Ibrahim, M. Negera, Melting and viscous dissipation effect on upper-convected Maxwell and Williamson nanofluid, Engineering Reports e12159 (2020).

[4] Nilankush Acharya, Suprakash Maity, Prabir K, Kundu, Differential transformed approach of unsteady chemically reactive nanofluid flow over a bidirectional stretched surface in presence of magnetic field, heat transfer Asian Research 49 (6) (September 2020) 3917–3942.

[5] Nilankush Acharya, Spectral quasi linearization simulation of radiative nanofluidic transport over a bended surface considering the effects of multiple convective conditions, European Journal of Mechanics - B/Fluids, Volume 84 (November–December 2020,) 139–154.

[6] H. Waqas, M. Imran, S.U. Khan, S.A. Shehzad, M.A. Meraj, Slip flow of Maxwell viscoelasticity-based micropolar nanoparticles with porous medium: a numerical study, Appl. Math. Mech. 40 (9) (2019) 1255–1268.

[7] Nilankush Acharya, Fazle Mabood, On the hydrothermal features of radiative Fe_3O_4–graphene hybrid nanofluid flow over a slippery bended surface with heat source/sink, J. Therm. Anal. Calorim. 143 (2021) 1273–1289.

[8] Nilankush Acharya, Raju Bag & Prabir Kumar Kundu, On the impact of nonlinear thermal radiation on magnetized hybrid condensed nanofluid flow over a permeable texture, *Applied*, Nanoscience 10 (2020) 1679–1691.

[9] Muhammad Sadiq Hashmi, Nargis Khan, Sami Ullah Khan, M. Ijaz Khan, Thermophoretic particles deposition features in thermally developed flow of Maxwell fluid between two infinite stretched disks, Journal of Materials Research and Technology, Journal of Materials Research and Technology, Volume 9, Issue 6, November–December 2020, Pages 12889-12898.

[10] Nilankush Acharya, Kalidas Das, Prabir Kumar Kundu, Outlining the impact of second-order slip and multiple convective condition on nanofluid flow: A new statistical layout, Can. J. Phys. 96 (2018) 104–111.

[11] M. Ijaz Khan, Transportation of hybrid nanoparticles in forced convective Darcy-Forchheimer flow by a rotating disk, International Communications in Heat and Mass Transfer, Volume 122, March 2021, 105177.

[12] G. K. Ramesh; G. S. Roopa; Sabir Ali Shehzad; S. U. Khan, Interaction of Al2O3-Ag and Al2O3-Cu hybrid nanoparticles with water on convectively heated moving material, Multidiscipline Modeling in Materials and Structures, vol. 16 No. 6, pp. 1651-1667, (2020).

[13] Khuram Rafique, Muhammad Imran Anwar, Masnita Misiran, Ilyas Khan, El-Sayed M. Sherif, The Implicit Keller Box Scheme for Combined Heat and Mass Transfer of Brinkman-Type Micropolar Nanofluid with Brownian Motion and Thermophoretic E_ect Over an Inclined Surface, Appl. Sci. 10 (2020) 280.

[15] A.V. Kuznetsov, Nanofuid bioconvection in water-based suspensions containing nanoparticles and oxytactic microorganisms: oscillatory instability, Nanoscale Res. Lett. 6 (2011) 100.

[16] O.D. Makinde, I.L. Animasaun, Bioconvection in MHD nanofluid flow with nonlinear thermal radiation and quartic autocatalysis chemical reaction past an upper surface of a paraboloid of revolution, Int. J. Therm. Sci. 109 (2016) 159–171.

[17] Nilankush Acharya, Kalidas Das, Prabir Kumar Kundu, Framing the effects of solar radiation on magneto-hydrodynamics bioconvection nanofluid flow in presence of gyrotactic microorganisms, J. Mol. Liq. 222 (October 2016) 28–37.

[18] Nilankush Acharya, Raju Bag, Prabir Kumar Kundu, Unsteady bioconvective squeezing flow with higher-order chemical reaction and second-order slip effects, heat transfer Asian Research,(2021), https://doi.org/10.1002/htj.22137.

[19] Khan MI Usman, F. Shah, S.U. Khan, A. Ghaffari, Y.-M. Chu, Heat and mass transfer analysis for bioconvective flow of Eyring Powell nanofluid over a Riga surface with nonlinear thermal features, Numer Methods Partial Differential Eq. (2020) 1–17, https://doi.org/10.1002/num.22696.

[20] S.Nadeem, Adel Alblawi, Noor Muhammad, Ibrahim M.Alarifi, Alibek Issakhov, M. T.Mustafa, A computational model for suspensions of motile micro-organisms in the flow of ferrofluid, Journal of Molecular Liquids, Volume 298, 15 January 2020, 112033.

[21] Bagh Ali, Sajjad Hussain, Yufeng Nie, Liaqat Ali, Shabih Ul Hassan, Finite element simulation of bioconvection and cattaneo-Christov effects on micropolar based nanofluid flow over a vertically stretching sheet, Chin. J. Phys. 68 (December 2020) 654–670.

[22] M. Turkyilmazoglu, Flow of a micropolar fluid due to a porous stretching sheet and heat transfer, Int. J. Non Linear Mech. 83 (2016) 59–64.

Further reading

[14] M. Ijaz Khan, Faris Alzahrani, Free convection and radiation effects in nanofluid (Silicon dioxide and Molybdenum disulfide) with second order velocity slip, entropy generation, Darcy-Forchheimer porous medium, Int. J. Hydrogen Energy 46 (1) (2021) 1362–1369.